Global Change Biology (2001) 7, 127–145

Partitioning net ecosystem carbon exchange with isotopic fluxes of CO_2

DAVID R. BOWLING*, PIETER P. TANS† and RUSSELL K. MONSON*
*Department of Environmental, Population, and Organismic Biology, University of Colorado, Boulder, CO 80309,
†Climate Monitoring and Diagnostics Laboratory, National Oceanic and Atmospheric Administration, Boulder, CO 80303, USA

Abstract

Because biological and physical processes alter the stable isotopic composition of atmospheric CO_2, variations in isotopic content can be used to investigate those processes. Isotopic flux measurements of $^{13}CO_2$ above terrestrial ecosystems can potentially be used to separate net ecosystem CO_2 exchange (NEE) into its component fluxes, net photosynthetic assimilation (F_A) and ecosystem respiration (F_R). In this paper theory is developed to partition measured NEE into F_A and F_R, using measurements of fluxes of CO_2 and $^{13}CO_2$, and isotopic composition of respired CO_2 and forest air. The theory is then applied to fluxes measured (or estimated, for $^{13}CO_2$) in a temperate deciduous forest in eastern Tennessee (Walker Branch Watershed). It appears that there is indeed enough additional information in $^{13}CO_2$ fluxes to partition NEE into its photosynthetic and respiratory components. Diurnal patterns in F_A and F_R were obtained, which are consistent in magnitude and shape with patterns obtained from NEE measurements and an exponential regression between night-time NEE and temperature (a standard technique which provides alternate estimates of F_R and F_A). The light response curve for photosynthesis (F_A vs. PAR) was weakly nonlinear, indicating potential for saturation at high light intensities. Assimilation-weighted discrimination against $^{13}CO_2$ for this forest during July 1999 was 16.8–17.1‰, depending on canopy conductance. The greatest uncertainties in this approach lie in the evaluation of canopy conductance and its effect on whole-canopy photosynthetic discrimination, and thus the indirect methods used to estimate isotopic fluxes. Direct eddy covariance measurements of $^{13}CO_2$ flux are needed to assess the validity of the assumptions used and provide defensible isotope-based estimates of the component fluxes of net ecosystem exchange.

Keywords: canopy conductance, carbon dioxide, eddy covariance, forest micrometeorology, net ecosystem exchange, stable isotopes

Received 24 January 2000; revised version received 29 June and accepted 27 August 2000

Introduction

Stable isotopes of carbon dioxide contain unique information about the biological and physical processes that exchange CO_2 between terrestrial ecosystems and the atmosphere. Photosynthesis discriminates against the heavier ^{13}C isotope in CO_2, preferentially fixing $^{12}CO_2$ into plant biomass, with a decrease in isotope ratio of leaf tissue of C3 plants of nearly 20‰ relative to atmospheric CO_2 (Farquhar *et al*. 1989). There is apparently no fractionation associated with mitochondrial respiration, and so the isotope ratio of respired CO_2 should reflect that of photoassimilated carbon, which is subsequently used for respiration (Lin & Ehleringer 1997; but see Duranceau *et al*. 1999). There can, however, be small variations in the carbon isotope ratios of various chemical components of leaves, litter and soil organic matter (Ehleringer *et al*. 2000; References therein); thus, the isotopic composition of respired CO_2 can vary from that expected on the basis of photosynthetic discrimination alone. Nevertheless, photosynthesis during day-

Correspondence and present address: D. Bowling, Department of Biology, University of Utah, 257 S 1400 E, Salt Lake City, UT 84112, USA, tel +1/(801) 581-8917 office +1/(801) 581-4665, e-mail bowling@biology.utah.edu

light hours leaves the air in and near terrestrial ecosystems enriched in $^{13}CO_2$, and respiration tends to dilute the air of the heavy isotope. This is apparent as a pronounced diurnal cycle in $\delta^{13}C$ at the ecosystem scale (Flanagan *et al*. 1996) and as a seasonal cycle at the global scale (Trolier *et al*. 1996).

In principle, these natural labels will allow us to independently estimate the fluxes of net photosynthesis (F_A) and ecosystem respiration (F_R). The sum of these opposing processes, net ecosystem CO_2 exchange (NEE = $F_R + F_A$, where upward CO_2 fluxes are considered positive), is now routinely measured at more than a hundred sites around the world. However, a mechanistic understanding of how photosynthesis and respiration respond to various environmental changes is difficult to achieve when only net fluxes are measured. Three measurement-based approaches are currently used to estimate F_R and F_A at the canopy level. These include scaling up soil, leaf, and stem chamber measurements (Ryan *et al*. 1996; Law *et al*. 1999), locating eddy covariance instruments below the canopy to directly measure soil respiration (Baldocchi *et al*. 1997, 2000), and estimating total ecosystem respiration flux based on regressions of nocturnal NEE vs. temperature (Goulden *et al*. 1996; many studies since). Each of these methods at present involves considerable uncertainty, and similar results from the different approaches have so far been difficult to obtain (Lavigne *et al*. 1997). Stable isotopes provide a unique and independent way to examine photosynthetic and respiratory fluxes.

Yakir & Wang (1996) used micrometeorological flux measurements and stable isotopes to separate NEE into photosynthetic and respiratory components in several crops, with simple canopy structure and minimal environmental heterogeneity. The objective of the present paper was to investigate the utility of such an approach in a complex natural system that includes variation in those parameters likely to influence photosynthetic discrimination and the isotopic nature of respired CO_2. For example, variation between species, between age classes, and with height in a canopy is now well-established in light, photosynthetic rate, stomatal and hydraulic conductance, leaf nitrogen, and foliar respiration (e.g. Brooks *et al*. 1991; Ellsworth & Reich 1993; Baldocchi & Collineau 1994; Yoder *et al*. 1994; Hubbard *et al*. 1999). Soil moisture varies spatially and can influence soil respiration rates significantly (Davidson *et al*. 1998), either directly or through differences in nutrient availability and microbial community structure. These factors are likely to influence photosynthetic and respiratory isotope effects within a forest and may substantially complicate isotope partitioning in a natural system.

In this study, equations are developed to separate NEE into its photosynthetic and respiratory components using estimates of the net exchange of $^{13}CO_2$. Canopy-scale fluxes of $^{13}CO_2$ are then described in a deciduous forest in eastern Tennessee, and some related assumptions from an earlier study addressed. The goal was not an extensive characterization of the factors influencing $\delta^{13}C$ of forest air, but rather to determine whether or not stable isotopic fluxes of $^{13}CO_2$ could be used to successfully partition NEE in a natural forest. Finally the measured isotopic fluxes are combined with relevant isotopic and meteorological information, and NEE partitioning is discussed in detail.

Theory

Conservation of mass for CO_2 and $^{13}CO_2$ is used to develop equations that can be used to partition net ecosystem exchange. This approach is identical in principle to, but different in final formulation from, those of Yakir & Wang (1996) and Lloyd *et al*. (1996). Standard definitions for isotopic composition ($\delta^{13}C$), isotope ratio (R), and photosynthetic isotope discrimination (Δ) from the biological (Farquhar *et al*. 1989) rather than geochemical (Ciais *et al*. 1995; Hoefs 1997) literature are used.

Net ecosystem exchange (NEE) is given by conservation of mass for total CO_2 (Wofsy *et al*. 1993)

$$\mathrm{NEE} = \rho\overline{w'C'} + \rho\frac{\mathrm{d}C}{\mathrm{d}t} = F_R + F_A \quad (1)$$

$$\rho\frac{\mathrm{d}C}{\mathrm{d}t} = \rho\frac{\mathrm{d}}{\mathrm{d}t}\int_0^{z_m} C(z)\mathrm{d}z \quad (2)$$

where $\rho\overline{w'C'}$ is total CO_2 flux (measured by eddy covariance), the overbar denotes Reynolds averaging, the primes denote fluctuations from this average, F_R is the total respiratory flux of CO_2 (from heterotrophs, roots, and stems), F_A the net photosynthetic assimilation of CO_2 (gross photosynthetic uptake – leaf respiration), and $\rho\mathrm{d}C/\mathrm{d}t$ the time rate of change of CO_2 mole fraction (C) between ground level (0) and the measurement height (z_m). (A list of symbols used is provided in Table 1.) The convention that upward scalar fluxes are positive is followed; hence, F_A is a negative number during the day. $\rho\mathrm{d}C/\mathrm{d}t$ is referred to as the storage flux of CO_2 and is important when atmospheric stability alters vertical mixing and allows the mean C in the canopy space to change. This term is obtained by measuring C at various heights in and above the canopy and using (2). Following Ruimy *et al*. (1995) and Lloyd *et al*. (1996), nocturnal foliar respiration is included in F_R, but daytime foliar respiration is included in F_A (net assimilation).

Conservation of mass for ^{13}C can be applied to expand both equations. Multiplying through by isotope ratio, the following mass balance equations for $^{13}CO_2$ are obtained

$$\rho\overline{w'(R_aC)'} + \rho\frac{d(R_aC)}{dt} = R_rF_R + F_A\frac{R_a}{1+\Delta} \quad (3)$$

$$\rho\frac{d(R_aC)}{dt} = \rho\frac{d}{dt}\int_0^{z_m} R_aC(z)dz \quad (4)$$

where $1+\Delta$ denotes the fractionation factor associated with net photosynthesis, and R_a and R_r refer to the isotope ratios of CO_2 in canopy air and respired CO_2, respectively. In (3), the left-hand terms represent the net ecosystem exchange of $^{13}CO_2$, which involve a net eddy flux $\rho\overline{w'(R_aC)'}$ and a storage flux (eqn 4) of $^{13}CO_2$. The use of absolute isotope ratio ($R = {}^{13}C/{}^{12}C$) introduces the approximation $[^{13}CO_2] \approx ({}^{13}C/{}^{12}C)^*$[total CO_2] (where [] denotes mole fraction), which involves an error of about 1.11% for $[^{13}CO_2]$ and is roughly constant with observed atmospheric variation in $\delta^{13}C$ and $[CO_2]$. Alternatively, the isotope ratio (and PDB standard) can be redefined relative to total carbon as $R = {}^{13}C/({}^{12}C + {}^{13}C)$, in which case the above relationships are exact (neglecting ^{14}C, Tans *et al*. 1993). It is assumed herein that canopy air forms the CO_2 substrate for photosynthesis, ignoring leaf boundary layer conductance. The assumption is also made that there is no fractionation associated with autotrophic or heterotrophic respiration for $^{13}CO_2$.

Dividing by the PDB isotope ratio standard, subtracting (1), and converting to conventional δ notation, ignoring terms in Δ^2 or smaller (Lloyd *et al*. 1996), the following is obtained

$$\underset{I}{\rho\overline{w'(\delta^{13}C_aC)'}} + \underset{II}{\rho\frac{d(\delta^{13}C_aC)}{dt}} = \underset{III}{\delta^{13}C_rF_R} + \underset{IV}{F_A(\delta^{13}C_a - \Delta)} \quad (5)$$

Although mass is still conserved by (1) and (5), when using δ notation terms I and II no longer equal the net ecosystem exchange of $^{13}CO_2$. Instead, their sum is the isoflux of $^{13}CO_2$, which can be pictured as the product of NEE (of total CO_2) and the isotopic composition (expressed in δ units) of that net exchange. This quantity will be consistently referred to as isoflux, where isoflux = eddy isoflux (term I) + storage isoflux (term II). Writing this explicitly,

$$\text{isoflux} = \delta^{13}C_r\,(F_R) + (\delta^{13}C_a - \Delta)F_A. \quad (6)$$

The eddy isoflux can be estimated using the flux-gradient method over appropriate sites (Yakir & Wang 1996), with hyperbolic relaxed eddy accumulation (Bowling *et al*. 1999b), or a combination of flask measurements and standard eddy covariance (Bowling *et al*. 1999a). The storage isoflux can be obtained using flask measurements to characterize vertical profiles of isotopic composition and CO_2. It is noted that Bowling *et al*. (1999a) interpreted isoflux (in δ units) incorrectly as the net ecosystem exchange of $^{13}CO_2$ (which they denoted ^{13}NEE), and similarly misinterpreted the eddy and storage isoflux terms. The use of R (eqns 3 and 4) instead of δ notation would avoid the subtle distinction between isoflux and net exchange of $^{13}CO_2$. However, for consistency with other CO_2 mass balance studies we report $^{13}CO_2$ exchange as an isoflux in this paper.

$\delta^{13}C_rF_R$ (term III) represents the net flux of $^{13}CO_2$ added to the atmosphere by the total respiration flux F_R having isotopic composition $\delta^{13}C_r$. We assume that a single isotopic composition can be found that is representative of all components of ecosystem respiration (Keeling 1958). The term $(\delta^{13}C_a - \Delta)F_A$ represents the $^{13}CO_2$ removed by photosynthesis, which is the total photosynthetic uptake F_A times the isotope ratio of that assimilated carbon. The isotope ratio of photosynthetically produced carbon is given by the source air ($\delta^{13}C_a$) modified by the discrimination (Δ) associated with photosynthesis. Discrimination is defined here as a positive number, e.g. for an atmosphere with composition −8‰ and a photosynthetic discrimination of +18‰, $F_A(\delta^{13}C_a - \Delta) = F_A(-8‰ - 18‰)$.

Lloyd *et al*. (1996) used a mass balance approach to develop similar equations. Their eqn 10 has been particularly helpful in determining the relative importance of photosynthesis, respiration, and turbulent transport of air into the canopy in controlling the isotopic composition of forest CO_2 (Lloyd *et al*. 1996; Flanagan *et al*. 1997). This is a useful concept which has shown how important both biological and physical (boundary-layer depth, turbulent mixing) effects are in controlling isotopic composition of CO_2 in the surface layer. However, Lloyd's approach requires several assumptions which are not always satisfied in a forest canopy, such as a well-mixed canopy air space, which in a large closed canopy is usually satisfied only in late afternoon (e.g. Buchmann *et al*. 1996), and the dominance of certain one-way flux terms over the net eddy and storage fluxes. Lloyd *et al*. (1996) examine these assumptions in detail.

There are also conceptual parameters in Lloyd's approach which are difficult to directly measure: F_{oi}, the mean one-way flux of CO_2 into the canopy, which may be complicated by coherent turbulence structure (Raupach *et al*. 1996) and sampling interval considerations (Lenschow *et al*. 1994), and in particular δ_o, the mean isotopic composition of air moving into the canopy. These parameters are included in the turbulent transport term in Lloyd's eqn 10, which is calculated as a residual from other measured and modelled data (Lloyd

Table 1 Symbols used in the text

a	carbon isotope fractionation resulting from diffusion of CO_2 in air (4.4‰)
b	intercept of a linear regression between $\delta^{13}C_a$ and C (‰)
b_R	carbon isotope fractionation resulting from carboxylation by Rubisco (27.5‰)
C, C_a	CO_2 mole fraction in ambient air (μmol mol^{-1})
C_i	CO_2 mole fraction in the intercellular air space, integrated over the canopy (μmol mol^{-1})
c_i	CO_2 mole fraction leaving the canopy (inside – Lloyd *et al*. 1996; μmol mol^{-1})
c_o	CO_2 mole fraction entering the canopy from above (outside – Lloyd *et al*. 1996; μmol mol^{-1})
c_p	specific heat of air at constant pressure (J g^{-1} K^{-1})
δ	isotope composition of CO_2 relative to *PDB* ($\delta_x = (R_x/R_{PDB} - 1) \times 1000$, ‰)
$\delta^{13}C$	carbon isotope composition of CO_2 (‰)
$\delta^{13}C_a$	$\delta^{13}C$ of ambient CO_2 (‰)
$\delta^{13}C_r$	$\delta^{13}C$ of total ecosystem respiration flux (Keeling plot intercept,‰)
δ_i	$\delta^{13}C$ of CO_2 leaving the canopy (inside – Lloyd *et al*. 1996;‰)
δ_o	$\delta^{13}C$ of CO_2 entering the canopy from above (outside – Lloyd *et al*. 1996;‰)
Δ	carbon isotope discrimination of net photosynthesis, integrated over the canopy (‰)
Δ_E	net ecosystem discrimination (includes photosynthesis and ecosystem respiration – Lloyd *et al*. 1996;‰)
Δ_e	net ecosystem discrimination (free troposphere vs. ecosystem respiration – Buchmann *et al*. 1998;‰)
Δ_{LF}	an estimate of Δ, equal to $\delta^{13}C_a - \delta^{13}C_r$ (Lloyd & Farquhar 1994;‰)
F_A	total ecosystem net photosynthetic assimilation flux (μmol CO_2 m^{-2} s^{-1}, by our sign convention F_A is negative during net uptake)
F_R	total ecosystem respiration flux (μmol CO_2 m^{-2} s^{-1}, always positive)
G	soil heat flux (W m^{-2})
g_c	stomatal conductance to CO_2, integrated over the canopy (mol m^{-2} s^{-1})
γ	psychrometric constant (kPa K^{-1})
H	sensible heat flux (W m^{-2})
L	Obukhov length (m)
LE	latent heat flux (W m^{-2})
m	slope of a linear regression between $\delta^{13}C_a$ and C (‰ mol μmol^{-1})
MO	Monin–Obukhov similarity theory
NEE	net ecosystem exchange of CO_2 (μmol CO_2 m^{-2} s^{-1}, negative during uptake)
isoflux	net isoflux of $^{13}CO_2$ (see text for discussion, μmol CO_2 m^{-2} s^{-1} ‰)
overbar ($\bar{x}$)	Reynolds average
PAR	photosynthetically active radiation (μmol m^{-2} s^{-1})
PM	Penman–Monteith
prime (x')	fluctuations from the Reynolds average
R	molar ratio of heavy to light isotope ($^{13}C/^{12}C$, dimensionless)
R_a	R of ambient CO_2 (dimensionless)
r_a	total aerodynamic resistance (s m^{-1})
r_m	aerodynamic resistance to momentum deposition (s m^{-1})
R_n	net radiation flux (W m^{-2})
R_r	R of total ecosystem respiration flux (dimensionless)
r_t	aerodynamic resistance to turbulent transport of scalars (s m^{-1})
ρ	air density (kg m^{-3})
s	slope of the saturation vapour pressure vs. temperature curve for water (kPa K^{-1})
t	time (s)
u*	friction velocity (m s^{-1})
VPD	vapour pressure deficit (kPa)
w	vertical wind velocity (m s^{-1})
z	height (m)
z_m	height of measurement (m)
[]	mole fraction

et al. 1996). Furthermore, the goal of separating of photosynthetic and respiratory fluxes cannot be achieved using Lloyd's equation alone.

Equations (1) and (6) form the basis of the present method to distill F_A and F_R from net flux and net isoflux measurements. The influence of turbulent transport is directly included in measured parameters. If the total integrated canopy photosynthetic discrimination (Δ) is known, two equations can be solved to obtain two unknowns, F_A and F_R, can be derived. Below, the procedure for obtaining each of the terms in these equations is detailed.

Methods

Site

This study was conducted during July 1999 at the Walker Branch Watershed, a deciduous forest in eastern Tennessee. Dominant species in the forest are oaks (*Quercus alba, Q. prinus*), maples (*Acer rubrum, A. saccharum*), tulip poplar (*Liriodendron tulipifera*), and various hickory (*Carya*) species. Full site details are available elsewhere (Baldocchi & Harley 1995). Water availability in the forest was relatively high throughout the study, as evidenced by numerous rain showers prior to and during the measurements.

Flux and storage measurements

Fluxes of CO_2, sensible heat, latent heat, and relevant forest meteorological parameters were measured from a 44-m tall instrument tower. This study is part of a long-term CO_2 exchange study, and the instrumentation used has already been described extensively (Baldocchi & Harley 1995; Greco & Baldocchi 1996; Baldocchi 1997). Briefly, CO_2 and H_2O fluxes were measured above the canopy every 30 min via the eddy covariance technique (using a SWS-211/3K sonic anemometer, Applied Technologies, Boulder, CO, and an open path infrared gas analyser; Auble & Meyers 1992), and vertical profiles of CO_2 mole fraction were used to estimate canopy storage. These fluxes were combined to calculate net ecosystem CO_2 exchange (NEE) as described above. Because nocturnal eddy covariance fluxes are underestimated at low u^* (Goulden *et al*. 1996), an attempt was made to apply a friction velocity (u^*) threshold to the present data. However, during the period in which the isotope data are likely to be biologically valid (perhaps 2 weeks before and after isotope measurements), insufficient data were available to confidently fill gaps resulting from removal of low u^* periods.

Isofluxes were estimated by combining fast (10-Hz) CO_2 time-series with a linear relation between $\delta^{13}C$ and CO_2 mole fraction (Bowling *et al*. 1999a)

$$\text{eddy isoflux} = \overline{\rho w'(\delta^{13}C_a C)'} = \overline{\rho w'\{(mC + b)C\}'} \quad (7)$$

CO_2 time-series were adjusted to constant density using 10-Hz water and temperature data prior to applying (7). The linear relation was used to predict the isotope ratio of CO_2 from measured CO_2 mole fractions at four heights (1.1, 9.4, 21.4, and 37.0 m), and storage isofluxes were calculated as described above. Net isoflux was computed by adding the eddy isoflux from (7) and the storage isoflux from (5).

Flask measurements

The relationship between isotopic composition and C was established by collecting air in glass flasks. On 16–17 July 1999, 61 100 mL glass flasks (described by Ehleringer & Cook 1998) were filled with air at two sampling heights. The goal was to evaluate the $\delta^{13}C$-vs.-C relationship at a variety of timescales, ranging from those characteristic of eddy covariance measurements (100 ms to 30 min) to those characteristic of standard isotopic flask sampling (tens of minutes). Timing of samples was chosen to represent photosynthetic and respiratory periods for all time scales.

Thirty-one flasks were filled by flushing with air at a flow rate of 280–300 mL min^{-1}, subsampling from air at 26.0 m height through 70 m of 0.64 cm ID Teflon tubing (PFA, Cavalier Components, Inc., Richmond, VA). Air was pulled quickly through the long sampling line; residence time in the Teflon tubing was 9 s, and the air in the flasks represented roughly a 20-s average at the sampling flow rate. The samples were dried using a $Mg(ClO_4)_2$ trap. These flasks, referred to as the 30-s timescale, were obtained roughly every 2–3 h over a 48-h period.

Eight flasks were filled at 37.0 m height to represent a 30-min time average by flushing air through a large glass volume (11.6 L) at 387 mL min^{-1}, through a $Mg(ClO_4)_2$ drying trap, then through a flask. These flasks, referred to as the 30-min timescale, were obtained on 16 July at 04.00, 09.00, 15.00, 20.00, and on 17 July at 04.00, 09.00, 14.00, and 20.00 hours (local standard time).

Twenty-two flasks were filled at 37.0 m by first evacuating to a pressure of 10^{-1} kPa, then immediately filling within 50 cm of the open path IRGA by activating a solenoid valve with a switch. Manometric laboratory tests with this system showed that the flasks filled to 63% (one time constant for an exponential process) of their final pressure within 427 ± 5 ms, and 100% pressure within 921 ± 7 ms (mean $\pm$ SE, $n = 10$). Further testing showed no fractionation when evacuated 100 mL flasks were filled from a 18.9-L glass volume rather than flushing the flasks; the measured difference in $\delta^{13}C$ of the large volume and the flasks was 0.01 ± 0.11‰ (mean $\pm$ SD, $n = 10$). It was impossible to dry the evacuated flask samples during collection, so appropriate mixing ratio corrections were applied as described below. These flasks are referred to as 500-ms timescale.

Carbon isotope ratios of CO_2 in the flasks were measured on a continuous-flow isotope ratio mass spectrometer (Finnigan MAT 252, San Jose, CA) as described by Ehleringer & Cook (1998). Precision for $\delta^{13}C$ was determined daily by injections of known standards ($n = 4$ or 5 each day) and was typically ± 0.06‰ ($n = 25$ overall). Appropriate corrections for

the presence of ^{17}O were applied, and CO_2 was separated from N_2O before analysis via gas chromatography. Mole fraction of CO_2 was determined by integrating the m/z 44 peak and comparing to injections from known standards, with a precision of $\pm 5.5\,\mu mol\ mol^{-1}$. This relatively large error for C results from variation in the 300 µL injection volume of a sample into the mass spectrometer. Corrections were made for water vapour in the 500 ms flasks using 10-Hz water vapour density data corrected to mean water vapour density at 36.0 m (HMP 35D humitter, Vaisala, Woburn, MA), and matched exactly in time to the flask sampling times. Differences in C between flasks resulting from errors in absolute water vapour density are at least an order of magnitude smaller than the precision of the C measurement.

Partitioning approach

Equations (1) and (6) are used to partition NEE into its components. In these equations respiration (F_R) and photosynthetic assimilation (F_A) fluxes are assumed to be unknowns, and the exchange terms (NEE and isoflux) are obtained as described above. $\delta^{13}C_r$, the isotope ratio of respired CO_2, was obtained using the Keeling-plot approach ($\delta^{13}C_r$ equals the intercept of a plot of $\delta^{13}C_a$ vs. the inverse of C on samples collected at night; Keeling 1958). The isotope ratio of atmospheric CO_2 ($\delta^{13}C_a$) was either directly measured or calculated from C measured at 22.0 m and the flask regression.

Δ is calculated using an equation developed at the leaf scale (Farquhar *et al*. 1982)

$$\Delta = a + (b_R - a)\frac{C_i}{C_a} \tag{8}$$

where a is the fractionation resulting from diffusion of CO_2 in air (4.4‰) into the leaf, b_R is the net fractionation of the enzyme-catalysed fixation (roughly 27.5‰) of CO_2, and C_i and C_a are the CO_2 mole fractions in the intercellular air space and ambient air, respectively. Note that in this equation C_i is integrated over the whole canopy, and the measured C at 22.0 m (near canopy top) is used for C_a. Although Lloyd *et al*. (1996) provide a useful formulation for integrating Δ over many canopy layers to provide a flux-weighted average discrimination, canopy-scale measurements in a big-leaf analogue model are used in preference here to estimate Δ via C_i obtained from the gas exchange relation

$$-F_A = g_c(C_a - C_i), \tag{9}$$

where g_c is the integrated canopy stomatal conductance to CO_2. (The negative sign on F_A is required by the sign convention used.) The four equations (1), (6), (8) and (9) contain five unknowns (F_A, F_R, Δ, C_i, and g_c). Provided that g_c is known, these equations can be combined to provide a quadratic equation which provides only one realistic solution for F_A (derived in the Appendix). F_R can then be found using (1).

g_c was calculated from measured parameters by inverting the Penman–Monteith (PM) equation (e.g. Grace *et al*. 1995)

$$\frac{1.6}{g_c} = \frac{s r_a (R_n - LE - G - H) + \rho c_p VPD}{\gamma LE} - r_a \tag{10}$$

where s is the slope of the saturation vapour pressure vs. temperature curve for water, R_n is net radiation, LE, G, and H are latent, soil, and sensible heat fluxes, ρ is air density, c_p is the specific heat of air, VPD is saturation vapour pressure deficit, γ is the psychrometric constant, and the 1.6 factor arises in the conversion from conductance of H_2O to CO_2. The aerodynamic resistance term r_a was computed as the sum of a resistance to momentum (r_m, which is a function of atmospheric stability) and an extra term (r_t) for turbulent transport of scalars using the approach of Magnani *et al*. (1998).

Δ was also estimated using a second approach. Evans *et al*. (1986) derived equations to calculate discrimination by a leaf enclosed in a cuvette based on the mole fraction and isotopic composition of CO_2 in the inlet and outlet air streams. Lloyd *et al*. (1996) suggested that this concept could be extended to the 'on-line' discrimination of an entire canopy

$$\Delta_E = \frac{-c_o(\delta_o - \delta_i)}{(c_o - c_i)} \tag{L15}$$

where c_o and c_i (δ_o and δ_i) represent the CO_2 mole fractions (isotope ratios) in air outside and inside the canopy air space, respectively. (Lowercase c_i and c_o are used here to distinguish from C_i developed earlier.) Combining Lloyd's equation with the Evans approach to calculate photosynthetic discrimination from Δ_E gives

$$\Delta = \frac{1000\left(\frac{c_o}{c_o - c_i}\right)(\delta_i - \delta_o)}{1000 + \delta_i - \left(\frac{c_o}{c_o - c_i}\right)(\delta_i - \delta_o)} \tag{EA15}$$

Notation in (EA15) is consistent with Lloyd *et al*. (1996) and differs from Evans *et al*. (1986). Herein c_o and c_i are estimated by averaging the 10-Hz CO_2 time series when $w' < 0$ (c_o) and $w' > 0$ (c_i), and derive δ_o and δ_i from c_o and c_i and the flask regression (Table 2), and refer to this as 'on-line' discrimination by analogy with leaf measurements. Note that estimation of δ_o and δ_i depends on the

Table 2 Geometric mean regressions of $\delta^{13}C$ vs. CO_2 and $1/CO_2$ for flask samples collected at varying temporal scales.

Flask type	m	b	r^2	n
$\delta^{13}C = mC + b$				
All flasks	−0.033 ± 0.002	2.92 ± 0.80	0.956	61
Night	−0.026 ± 0.003	−0.32 ± 1.35	0.948	15
Day[1]	−0.039 ± 0.005	5.23 ± 1.91	0.849	46
30 min	−0.036 ± 0.003	4.06 ± 1.16	0.991	8
30 s	−0.033 ± 0.003	2.85 ± 1.22	0.959	31
500 ms	−0.033 ± 0.004	3.02 ± 1.57	0.943	22
$\delta^{13}C = m(1/C) + b$				
All flasks	5962 ± 314	−25.30 ± 0.79	0.962	61
Night[2]	5756 ± 953	−24.87 ± 2.16	0.918	15
Day	5772 ± 714	−24.80 ± 1.87	0.845	46
30 min	5696 ± 306	−24.68 ± 0.79	0.996	8
30 s	6091 ± 410	−25.68 ± 1.02	0.970	31
500 ms	5550 ± 619	−24.14 ± 1.59	0.943	22

[1]This regression was used to compute $^{13}CO_2$ fluxes (eqn 7).
[2]The intercept of this regression was used as $\delta^{13}C_r$.

linear relation $\delta = mC + b$, and at present δ_o and δ_i are impossible to measure directly.

All measured and derived parameters were calculated every 30 min over a 19-day period (13 July to 31 July 1999). There can be significant run-to-run variability in measured fluxes associated with footprint changes, nonstationarity of atmospheric turbulence, complex topography, inadequate sampling interval, and other factors (Moncrieff *et al*. 1996; Blanken *et al*. 1998). Application of this partitioning approach to individual half-hour periods proved problematic and sometimes resulted in unrealistic magnitudes for F_R and F_A, and errors in eddy covariance measurements are difficult to assess for individual sampling intervals anyway. Results are presented as ensemble-averages of each half-hour period over the 19-day time period, but note that the partitioning approach was always applied to the half-hour data.

Results and discussion

Relationship between $\delta^{13}C$ and C

It is firmly established in the literature that $\delta^{13}C$ and the inverse of C tend to be linearly related (Keeling 1958; numerous studies since). However, plots of $\delta^{13}C$-vs.-C are also linear at the ecosystem and regional scales (Friedli *et al*. 1987; Flanagan *et al*. 1996; Nakazawa *et al*. 1997a,b; Bowling *et al*. 1999a). Bowling *et al*. (1999a) exploited this relationship to estimate $^{13}CO_2$ fluxes. A critical and untested assumption of their approach is that the linear relation holds at all time scales important to turbulent transport of mass (roughly 100 ms to 30 min). Bowling *et al*. (1999a) used the hyperbolic relaxed eddy accumulation (HREA) technique to collect updraft and downdraft air for isotopic analysis, and showed that while the $\delta^{13}C$-vs.-C relation is linear for both flask (whole-air) and HREA (updraft or downdraft samples), the slopes and intercepts for each type of sample were not the same. This raises the question of whether the application of (7) to 10-Hz flux data is appropriate.

The relationship between carbon isotopic composition and CO_2 mole fraction at Walker Branch in July 1999 is shown in Fig. 1(a). Samples were collected on timescales that varied by more than three orders of magnitude, and the relation does not show the significant change in slope apparent in the HREA samples of Bowling *et al*. (1999a). Regressions for these samples are shown in Table 2. This constitutes strong evidence that the $\delta^{13}C$-vs.-C linearity holds at short timescales, and thus application of (7) for $^{13}CO_2$ appears legitimate. The variation in slope between analyses conducted by HREA vs. flask sampling that was observed in our previous study (Bowling *et al*. 1999a) must be a consequence of factors other than timescale incompatibility.

The $\delta^{13}C$-vs.-C regressions for the daytime and nighttime samples differ significantly. This is important because the nocturnal mixing line represents the influence of respiration alone, while the daytime relation shows the combined effects of photosynthetic discrimination and respiration. This was noted by Bowling *et al*. (1999a) and is apparent in figs 7 and 8 of Flanagan *et al*. (1996), which included only nocturnal data. However, because the isotope ratio of forest CO_2 is strongly influenced by atmospheric stability, the daytime (nighttime) influence may persist into the early evening (morning). Flanagan's plots do include measured C in the range of 360–390 μmol mol^{-1}, which likely include the photosynthetic influence.

$\delta^{13}C$ is plotted vs. $1/C$ in Fig. 1(b), and separated into day and night periods, based on an arbitrary day/night division of –11‰ (see also Fig. 3c). The intercept of a regression of the nocturnal data is commonly interpreted as the isotope ratio of respired CO_2, integrated over the whole ecosystem (Keeling 1958). A fundamental limitation of the Keeling-plot approach is evident in the figure; the intercept is extrapolated far beyond the region that includes measurements, and small errors in determination of the slope lead to amplified errors in the intercept (Buchmann *et al*. 1988). Dashed lines represent the 95% confidence intervals on the nocturnal regression slope, and lead to a range in estimated $\delta^{13}C_r$ of –22.7 to –27.0‰. In the present partitioning exercise the regression intercept of –24.9‰ is used.

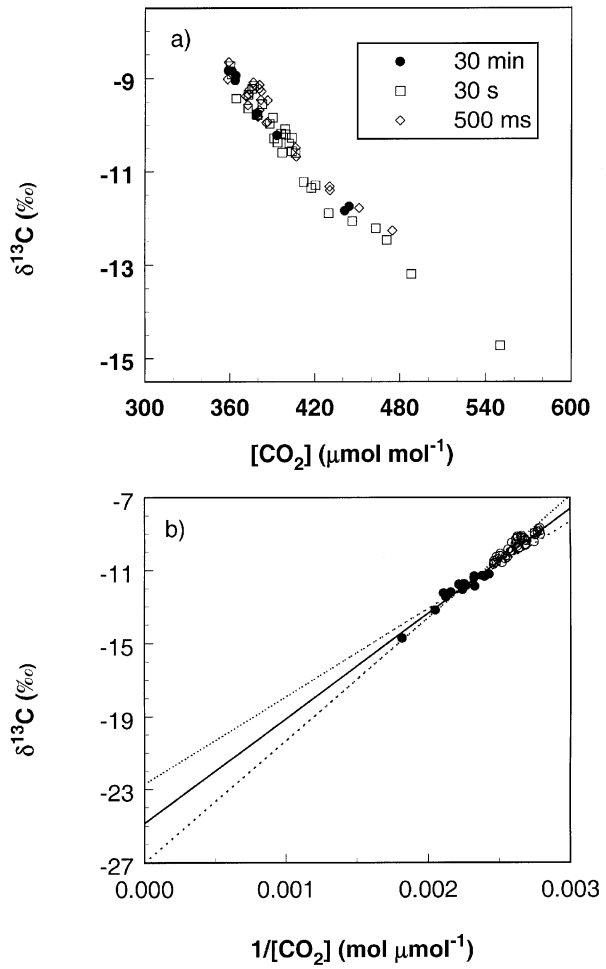

Fig. 1 (a) $\delta^{13}C$ of forest CO_2 vs. CO_2 mole fraction for flask samples collected at a variety of timescales. The 500-ms data have been corrected for the presence of water vapour in the flasks as described in the text; other samples were dried during collection. Samples were collected at heights of 37 m (30-min and 500-ms) and 26 m (30 s) above the ground; forest canopy height was 26–28 m (b) A Keeling plot of the same data, separated into day (open circles) and night (filled circles) periods. The solid line is a geometric mean regression of the night-time data, and the dashed lines are the 95% confidence intervals on the slope. Equations for the regressions are shown in Table 2.

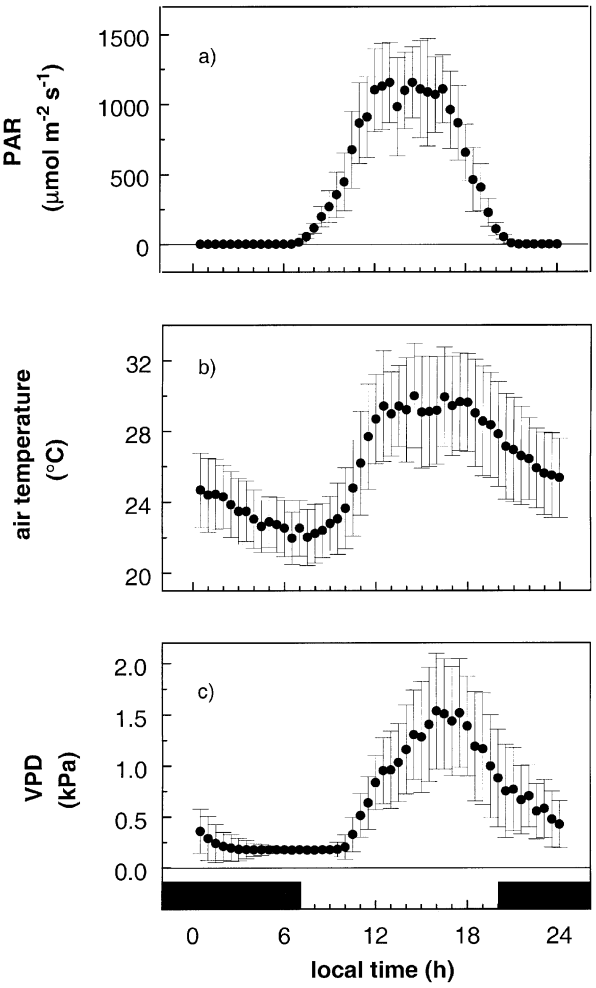

Fig. 2 (a) Mean photosynthetically active radiation (b) mean air temperature, and (c) mean vapour pressure deficit. Data points in this figure (and in Figs 3–9) are means, and error bars are 1 SD of each quantity every half-hour during 13–31 July 1999. Dark panels in this and subsequent figures denote nocturnal periods.

Environmental parameters, NEE, and $\delta^{13}C_a$

Nineteen-day ensemble averages of environmental parameters are shown in Fig. 2. PAR peaked on average about 1150 μmol m^{-2} s^{-1}, and mean air temperature during the study ranged from 22 to 30 °C. High evaporative demand was apparent most afternoons as mean *VPD* approached 1.5 kPa. Averages of NEE, isoflux, and $\delta^{13}C_a$ are shown in Fig. 3. These are the relevant measured parameters in the partitioning equations (1) and (6). There was significant day-to-day variability in the fluxes, but consistent diurnal patterns were observed. Similar variability has been observed in most eddy covariance studies (e.g. Moncrieff *et al*. 1996; Yang *et al*. 1999) but error bars are often reported as standard error rather than standard deviation. NEE peaked on average at about –23 μmol m^{-2} s^{-1}, typical for this forest when water is not limiting (Baldocchi 1997). The release of stored respiratory CO_2 in the morning hours was apparent as strong negative storage flux (Fig. 3a). Patterns for isoflux are similar (Fig. 3b), with a mid-day peak of 620 μmol m^{-2} s^{-1} ‰. The isoflux is not simply a linear function of NEE as might be expected from (7) (discussed below). The strong opposing influences of respiration and photosynthesis on forest air are apparent (Fig. 3c). CO_2 was consistently depleted in the

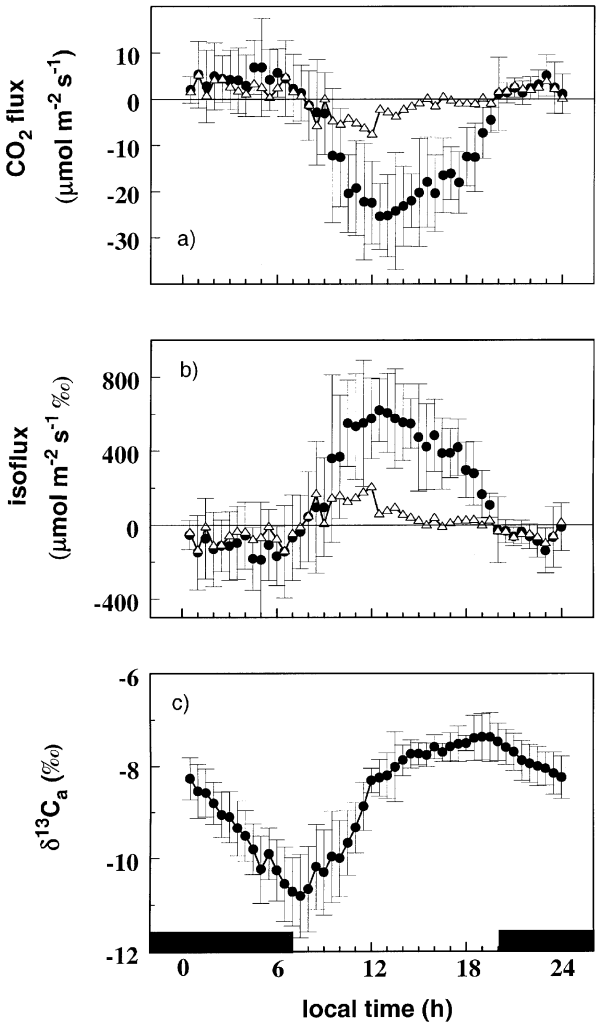

Fig. 3 (a) Mean NEE (circles) and storage flux (triangles) of total CO_2, (b) mean net isoflux (circles) and storage isoflux (triangles) of $^{13}CO_2$, and (c) mean $\delta^{13}C$ of CO_2 at 22 m ($\delta^{13}C_a$). Note that the true direction of the $^{13}CO_2$ flux is downward during photosynthetic periods. The isoflux associated with the net uptake of $^{13}CO_2$ is positive.

heavier ^{13}C isotope (more negative $\delta^{13}C$) in the early morning and enriched in late afternoon.

Canopy conductance

In order to use the isotope data to estimate F_A and F_R fluxes, knowledge of canopy-integrated photosynthetic discrimination is required, which, in turn, is dependent on mean canopy conductance. Canopy conductance was calculated for the study period (Fig. 4) and is similar in magnitude to conductances derived for other temperate deciduous forests (Kelliher *et al*. 1995). The diurnal pattern in g_c generally follows available energy (plotted as net radiation in Fig. 4). However, there is considerable

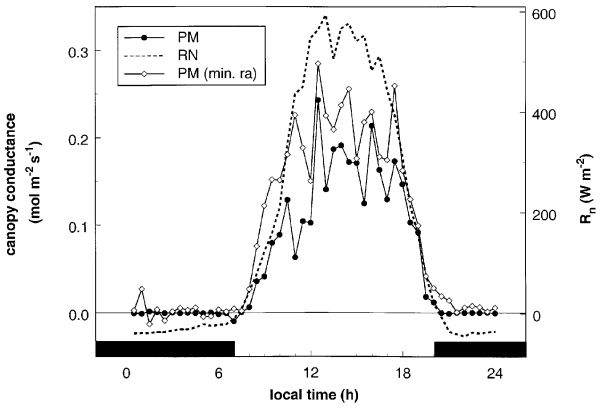

Fig. 4 Mean canopy conductance calculated from measurements by inverting the Penman–Monteith equation using a stability-dependent (PM, circles) and a minimum value (PM (min. r_a), diamonds) for aerodynamic resistance. Mean net radiation (R_n) is shown for comparison. Error bars are omitted for clarity.

variation in the conductance estimate derived from the PM equation, which does not appear to be driven by changes in available energy. Day-to-day variability in conductance was high (not shown, but see error bars in Fig. 5d) leading to large scatter in the mean values of Fig. 4. This scatter represents natural variability in LE and VPD and should not be interpreted as a consistent trend in g_c. Such variability is problematic for an accurate determination of Δ, and the causes of the variation deserve further scrutiny.

Various mean atmospheric parameters are shown in Fig. 5. Aerodynamic resistance to both momentum (r_m) and scalar (r_t) transport was significant at night and in the early morning hours, and controlled the timing of the rise of the PM-derived canopy conductance (Fig. 4). Note that these terms are not completely zero even during well-mixed afternoon conditions. When r_a ($= r_m + r_t$) is forced to equal the minimum observed mid-day value (23.1 s m^{-1}, Fig. 5a) at all times of the day, the PM-derived g_c rises earlier and peaks substantially higher (Fig. 4). The 'correct' conductance is likely to be intermediate in magnitude between these estimates. Inversion of the PM equation to estimate conductance assumes accurate energy balance closure, but in the present dataset the sum of latent and sensible heat, soil heat flux, and canopy/soil heat storage accounted for only 82% of incoming energy (this is typical at Walker Branch; Wilson & Baldocchi 2000). Further, the logarithmic wind profile on which r_m is based is complicated by canopy roughness, and transfer resistance (r_t) is modelled using Monin–Obukhov (MO) similarity theory (Magnani *et al*. 1998), which may not hold at all times of the day (discussed below). As will be shown, these uncertainties in the determination of g_c, and their effect on Δ, directly

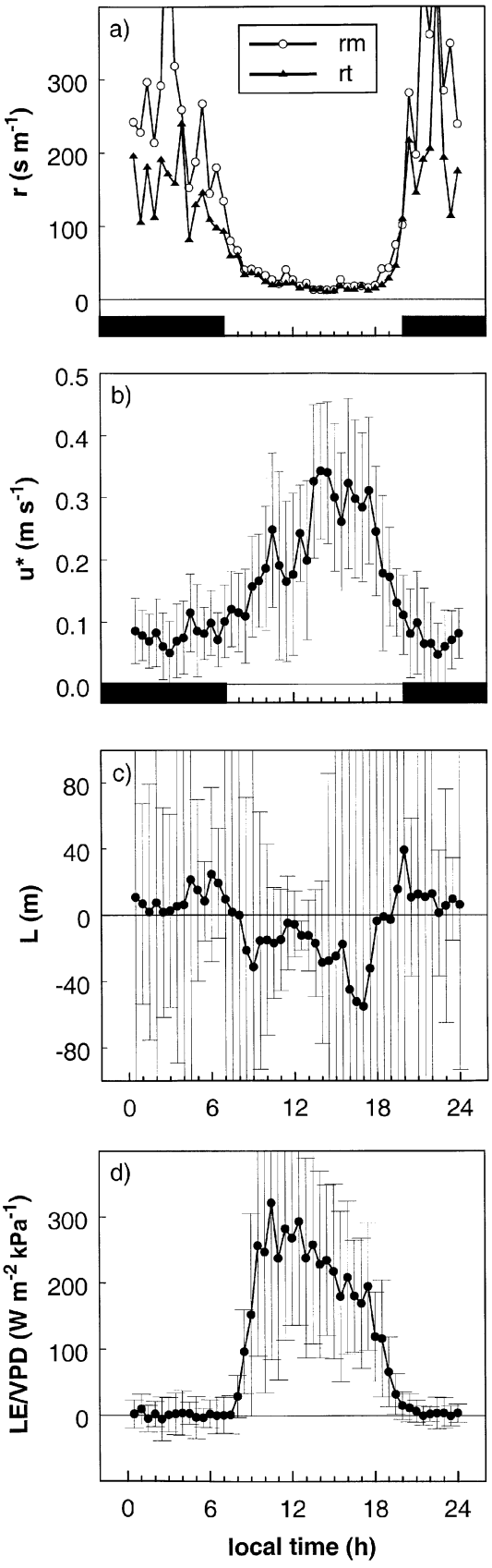

affect the F_A and F_R fluxes derived from NEE and isoflux. Correct evaluation of g_c is therefore necessary for accurate NEE partitioning.

Surface heating and associated turbulence began (shown by increased friction velocity in Fig. 5b) at sunrise, and continued monotonically until about 10.30 hours. This was followed by a 2.5-h period where u^* no longer increased. The Obukhov length (L) is a commonly used scaling variable in the atmospheric surface layer, and is an indicator of the relative importance of buoyant vs. mechanical production of turbulence. During this time period, L became small and negative, with substantially lower day-to-day variability than during other periods (Fig. 5c). This indicates strong buoyant turbulence, and vertical mixing associated with free convection (which usually involves the failure of MO similarity theory and hence our formulation for r_t is questionable during this period). Latent heat flux and vapour pressure deficit (VPD) at this time continued to increase, but at different rates (data not shown). Increases in latent heat flux may result from upward-moving moist air or downward-moving drier air (or both), and are not necessarily an indicator of continually increasing transpiration by the vegetation. This phenomenon is apparent as a sharp decrease in the mean ratio LE/VPD in Fig. 5(d) near 11.00 hours, and translates to a strong dip in the PM-derived conductance (Fig. 4, eqn 10). Whether or not this change is a realistic indicator of a physiological change in stomatal conductance (and thus Δ) is a critical and difficult question. Stomata clearly respond to changes in atmospheric moisture, but this occurs in the leaf boundary layer and may be fully decoupled from the atmosphere (Jarvis & McNaughton 1986). Because the sawtooth patterns of the PM-derived conductances in Fig. 4 likely do not reflect true leaf-level physiological changes, it is assumed that their general magnitude and diurnal shape are correct, and mathematically smoothed conductances derived from each (as well as the originals) are used in our partitioning exercise. These smoothed conductances are shown in Fig. 6. Also shown in Fig. 6 is a conductance estimate derived from the 'on-line' discrimination approach [Δ was prescribed by eqn EA 15, and g_c was then calculated by first solving (1) and (6) for F_A, then using (8) and (9)]. This conductance is similar in rise time and pattern to the PM conductance (but without the dip during boundary-layer growth), and declines more rapidly in the afternoon. The 'on-line' conductance

Fig. 5 (a) Mean aerodynamic resistance to momentum (r_m, circles) and scalar (r_t, triangles) transport, (b) mean friction velocity (u^*), (c) mean Obukhov length (L), and (d) mean ratio of latent heat flux to vapour pressure deficit (LE/VPD).

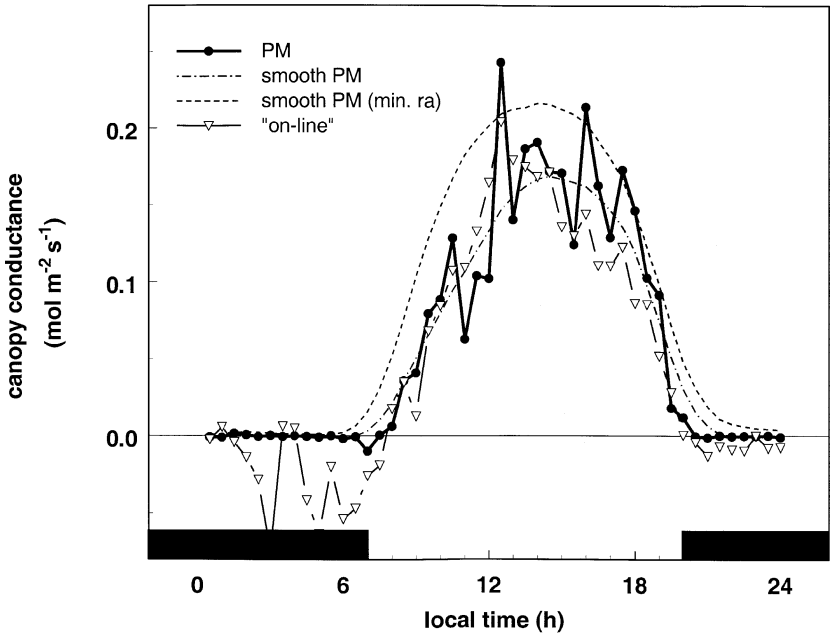

Fig. 6 Mean canopy conductance (PM, repeated from Fig. 4 for comparison), mathematically smoothed canopy conductance for both the stability-dependent (smooth PM) and minimum aerodynamic resistance (smooth PM (min. r_a)) cases, and canopy conductance calculated using the canopy-level 'on-line' discrimination estimate.

estimate is based on changes in C (and $\delta^{13}C$) rather than changes in water vapour flux. The difference in the PM and on-line g_c may indicate temporal changes in water use efficiency (F_A/LE) at the canopy scale. Alternatively, the difference may indicate that water vapour concentrations and fluxes are more affected by mixing of air from above the forming boundary layer than are CO_2 concentrations and isotope ratios.

Isotope partitioning

The partitioning results are summarized in Fig. 7. Measured NEE is shown in each panel for comparison. Regressions of nocturnal NEE vs. soil or air temperature (derived during windy periods) are often used in eddy covariance studies to estimate total ecosystem respiration flux, and net assimilation is calculated as a residual [$F_A = \mathrm{NEE} - F_R(T)$, Goulden *et al*. 1996]. The present isotope-derived estimates of F_R and F_A are compared to those based on the regression reported for Walker Branch by Greco & Baldocchi (1996) as an independent estimate of respiration flux (Fig. 7). It should be stressed that the temperature-based regressions are noisy and considerable variation is apparent in measured NEE at night that cannot be explained by temperature variation (Goulden *et al*. 1996). Thus these temperature-based fluxes are not necessarily the 'correct' respiration fluxes, but are a useful measure for comparison.

Shown in Fig. 7(a) are the fluxes obtained by using the PM-derived conductance in Fig. 4. Considerable scatter is propagated to the fluxes from the g_c scatter, and respiration fluxes are erroneously negative at midmorning. As discussed, the dip in g_c during this period (10.30–12.00 hours) likely does not reflect actual physiological changes in conductance of the forest. Photosynthesis is underestimated during this period and hence respiration becomes negative to compensate (eqn 1). When the scatter in canopy conductance is removed by smoothing, resulting F_A and F_R fluxes appear more realistic (Fig. 7b). Photosynthetic flux peaks at solar noon as would be expected from leaf-level light response curves (note that NEE in the present data does not peak at solar noon), but the respiration flux remains negative during the morning transition.

As mentioned, the formulation of aerodynamic resistance strongly controls the dynamics of the rise in g_c (Fig. 4). If the present estimates for r_a were smaller, g_c would rise earlier in the day and F_A would be proportionally larger (eqn 10). Using the mid-day minimum value for r_a (Fig. 4) at all times of the day indeed increases the magnitude of the fluxes but results remain noisy (Fig. 7c). Smoothing g_c results in much smoother F_R and F_A fluxes (Fig. 7d) as expected. Nocturnal NEE and F_R in Fig. 7(d) are very similar, and the daytime F_R is higher than would be predicted from regression based on temperature. Photosynthetic flux peaks prior to solar noon.

The 'on-line' estimate of g_c is based on CO_2 instead of H_2O measurements. Partitioning results using this g_c are shown in Fig. 7(e). Respiration fluxes appear to be underestimated during most of the day, implying the relatively small conductance forces F_A to be too small.

The dynamics of the rise in conductance are similar in the 'on-line' and standard PM cases (Fig. 6), and the 'on-line' estimate is lower in the afternoon.

The actual canopy conductance is likely to be intermediate between the standard PM case and the case involving minimum aerodynamic resistance, and hence the correct assimilation and respiration fluxes are likely intermediate between Fig. 7(b),(d).

By treating the canopy as a single layer to determine canopy conductance and Δ, well-established complexity in vegetation canopies is explicitly ignored. Many studies have shown that vertical gradients exist in those factors controlling leaf stomatal conductance: light availability, C_a (and $\delta^{13}C_a$), leaf temperature, saturation deficit, and photosynthetic capacity, C_i/C_a (and thus Δ) of individual leaves (Garten & Taylor 1992; Ellsworth & Reich 1993; Roden & Pearcy 1993; Brooks *et al.* 1997; see also References in Jarvis & McNaughton 1986). The degree to which these variations in physiology integrate to the canopy level is not well understood. Further, use of the PM equation to determine a bulk canopy conductance to CO_2 and its isotopes is complicated by the different roles of the soil in evaporative and CO_2 fluxes (Raupach & Finnigan 1988). Soil evaporation at Walker Branch in the

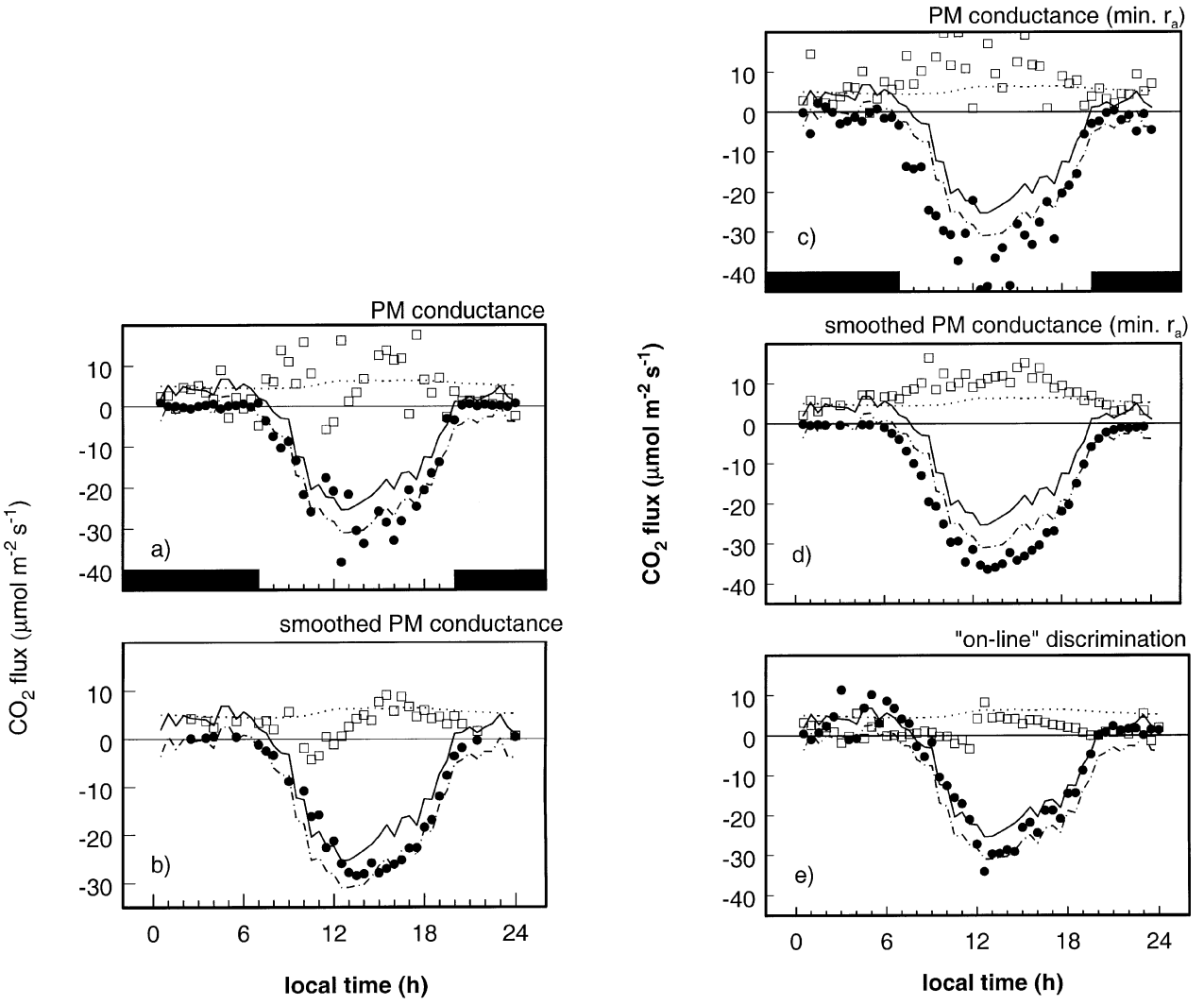

Fig. 7 Photosynthesis (F_A, circles) and respiration (F_R, squares) fluxes calculated from measured NEE (solid lines), isoflux, $\delta^{13}C_r$, and $\delta^{13}C_a$, using (1) and (6). Each panel is associated with a canopy conductance in Figs 4 or 6, and a relevant discrimination (Δ) in Fig. 9, through (8) and (9). Dotted lines represent respiration flux estimated from an exponential relationship between nocturnal NEE and air temperature (Greco & Baldocchi 1996), and the dashed-dotted lines are the derived photosynthetic fluxes calculated as $F_A = NEE - F_R(T)$. Solar noon during this period was approximately 14.10 hours.

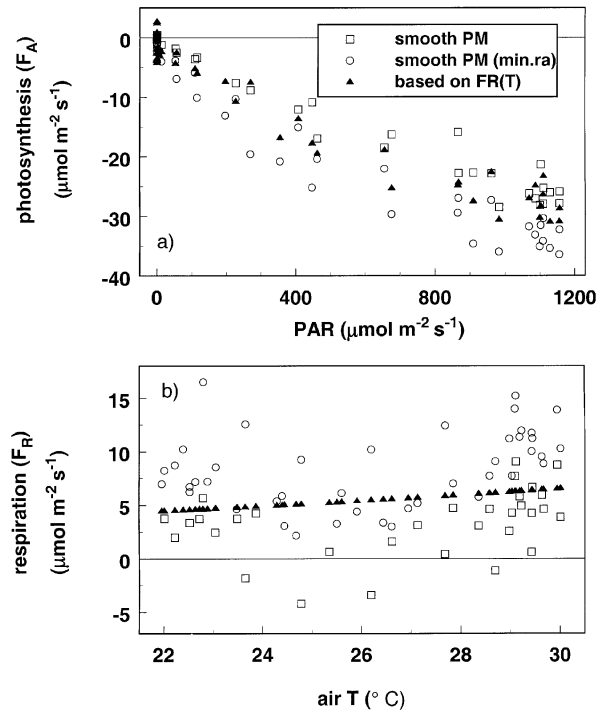

Fig. 8 (a) Light-response curves for whole-canopy photosynthesis (F_A) using the two smoothed estimates of canopy conductance and the temperature-based relation shown in Fig. 7. (b) Temperature-response curves for ecosystem respiration (F_R) for each case.

summer is a minimal component of evapotranspiration unless the litter is wet (Wilson *et al*. 2000), but soil CO_2 fluxes are generally a major component of total CO_2 flux regardless of litter moisture. Thus g_c may or may not be a realistic indicator of leaf-level properties.

Errors associated with the single-layer approach used herein are difficult to assess at this point. Advances have been made with other approaches to estimating whole canopy conductance (Granier *et al*. 2000) and these might provide better estimates of Δ. However, current global-scale carbon balance models incorporate photosynthetic discrimination (Ciais *et al*. 1995; Fung *et al*. 1997; Randerson *et al*. 1998; Bousquet *et al*. 1999) at a very simple level. While more accurate determinations of whole-canopy Δ are certainly desirable, they may be impractical to apply to global carbon cycle studies. Addition of leaf-level isotopic concepts to multilayer canopy physiology models (Baldocchi & Meyers 1998) and using Lagrangian approaches to modelling canopy resistances (McNaughton & van den Hurk 1995) and isotopic exchange (Raupach 2000) are important directions for future research. Such information may provide an understanding of whole-canopy discrimination patterns that proves practical for use in both canopy exchange and large-scale carbon cycle studies.

Despite these issues, expected diurnal patterns and magnitudes for the fluxes were obtained, and the results are consistent with our physiological understanding of leaf-level physiology and isotope discrimination. Yakir & Wang (1996) reported only mid-day values for their isotope-derived fluxes, and it was unclear whether the temporal dynamics of these fluxes could be resolved with stable isotopes. The present results suggest that stable isotopic studies offer the potential for improving our understanding of carbon and water relations at the ecosystem scale.

Light and temperature response

At the leaf scale, photosynthesis responds linearly to low light availability but saturates at higher light (Larcher 1995). At the canopy scale, the response of net CO_2 flux or NEE to light tends to be more linear (Grace *et al*. 1995; Ruimy *et al*. 1995; Greco & Baldocchi 1996; but see Hollinger *et al*. 1994; Malhi *et al*. 1998). Light response curves for NEE at Walker Branch tend to be more linear than most sites (Baldocchi 1997), and the isotope-derived photosynthetic fluxes are in agreement (Fig. 8a). Light levels at Walker Branch, however, can be much higher (1700 μmol m^{-2} s^{-1}) than observed herein (Baldocchi 1997), and the curves used herein do suggest a trend towards saturation at the highest light intensities.

When evaluated against air temperature, the isotope-derived respiration fluxes are quite variable (Fig. 8b), and do not closely follow the regression of Greco & Baldocchi (1996). The bi-modal distribution of the largest F_R fluxes (smooth PM, min r_a, circles) results from the pattern of respiration shown in Fig. 8(d), with morning (09.00 hours) and late afternoon (16.00) peaks. r_a is of greater importance at 09.00 than at 16.00 (Fig. 5a), and a value for r_a between that shown in Fig. 5(a) and the minimum value would result in F_R fluxes at 09.00 that are intermediate between those shown in Fig. 7(b),(d). Note that F_R fluxes around 09.00 are likely underestimated in Fig. 7(b) and overestimated in Fig. 7(d). Thus the formulation of r_a strongly influences the fluxes calculated by the present isotope approach.

Photosynthetic discrimination

In reality it is a measure of Δ (and not g_c) that needs to be used in (1) and (6) to partition NEE into F_R and F_A. If this parameter could be measured or modelled with confidence, then assessment of g_c would be unnecessary. Leaf-level discrimination (integrated over the lifetime of a leaf) has long been estimated by comparing the isotope

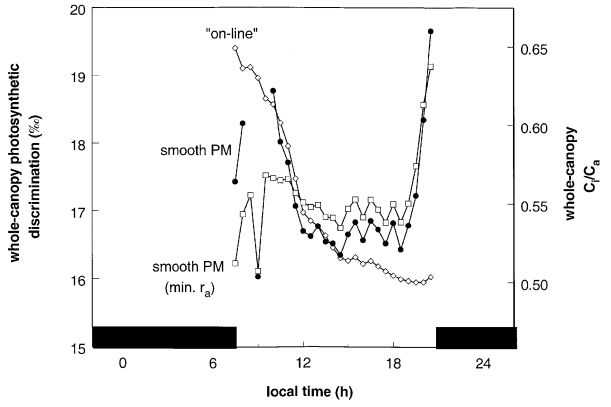

Fig. 9 Canopy-integrated photosynthetic discrimination (Δ) against $^{13}CO_2$ during daylight hours, and the canopy-integrated ratio of intercellular to ambient CO_2 mole fraction (C_i/C_a) calculated using (8).

Table 3 Average whole-canopy integrated photosynthetic discrimination (Δ), weighted by photosynthetic assimilation flux ($\Delta = \Sigma\ (\Delta x F_A)/\Sigma\ (F_A)$) and by NEE ($\Delta = \Sigma\ (\Delta x NEE)/\Sigma$ (NEE)). The NEE-weighted $\delta^{13}C_a$ value of –8.00 was used to compute Δ_{LF}, and the error estimate includes error in $\delta^{13}C_a$ and $\delta^{13}C_r$ from Table 2.

	Weighted by	
Conductance type	F_A (‰)	NEE (‰)
PM	16.9 ± 3.8	16.9 ± 2.8
Smoothed PM	16.8 ± 4.7	16.9 ± 2.6
PM (min. r_a)	17.1 ± 3.4	17.1 ± 2.8
Smoothed PM (min. r_a)	17.1 ± 3.5	17.1 ± 2.8
'on-line'	16.8 ± 3.6	16.8 ± 2.7
$\Delta_{LF} \approx \delta^{13}C_a - \delta^{13}C_r$	–	18.1 ± 3.0

ratios of air and of leaf biomass (Farquhar *et al*. 1989). However, instantaneous discrimination values can differ substantially from the integrated estimate (Brooks *et al*. 1997), and there is considerable variation in carbon isotope ratio of leaf biomass in this deciduous forest (Garten & Taylor 1992).

Δ in (6) represents the canopy-integrated photosynthetic discrimination against $^{13}CO_2$, and is analogous to discrimination by a leaf. This is the same discrimination described by Lloyd & Farquhar (1994) and Fung *et al*. (1997), applied in the present case on a smaller scale. Δ has been approximated as $\Delta_{LF} \approx \delta^{13}C_a - \delta^{13}C_r$ by Lloyd & Farquhar (1994), Flanagan *et al*. (1996), and Bakwin *et al*. (1998). The mathematical difference is stressed between Δ and other ecosystem discrimination values in the literature (Δ_e of Buchmann *et al*. (1998), which describe the difference in isotopic composition of ecosystem respiration and the free troposphere, and Δ_E of Lloyd *et al*. (1996), which represents the combined influences of photosynthetic and (both) autotrophic and heterotrophic respiratory fluxes on canopy (air). The formulations of large-scale inversion models (Ciais *et al*. 1995; Francey *et al*. 1995; Bousquet *et al*. 1999) use Δ, not Δ_e or Δ_E. There are currently no direct measurements of Δ at the canopy scale.

Discriminations associated with each conductance are shown in Fig. 9. Notable are the strong diurnal patterns, with higher discrimination in the early morning and lower discrimination in the afternoon. Patterns are similar for Δ derived from both water vapour (PM) and carbon dioxide ('on-line') measurements. These diurnal changes in discrimination are required to produce realistic diurnal patterns in F_A and F_R. Discrimination values at night were scattered and omitted from Fig. 9 (because there is no photosynthetic flux at night these values are irrelevant anyway). In the partitioning used herein night-time discrimination values are included to avoid artificially equating NEE and F_R, and the solutions of (1), (6), (8) and (9) generally force F_A to zero at night (Fig. 7).

These discrimination estimates are lower than expected. C3 plants generally have C_i/C_a near 0.6–0.9, corresponding to a photosynthetic discrimination of 18–24‰ (Farquhar *et al*. 1989). At present there are few experimental data with which to compare these results. The authors know of only one study in which photosynthetic discrimination was directly measured under ambient conditions in the field (at the leaf level, Harwood *et al*. 1998). Their results showed a general trend of higher discrimination in the morning and lower in the afternoon, with considerably larger overall diurnal change (from –30 to –15‰ over the day). Lloyd *et al*. (1996) used a model to estimate ecosystem F_R, then used an approach similar to the present one to derive Δ. Their results were quite similar in magnitude and diurnal pattern for a tropical forest (–20 to –18‰) but fairly noisy (–20 to –16‰) for a coniferous forest in Siberia. Trends in C_i/C_a for the present study (higher in the morning, lower in the afternoon) are consistent with those obtained in leaf-level studies of mid-day stomatal closure (e.g. Tenhunen *et al*. 1984; Kòppers & Schulze 1985).

The isotope ratio of respired CO_2 ($\delta^{13}C_r$) represents a production-weighted average of all organic carbon being metabolized in the ecosystem, and the heterotrophic component should integrate carbon fixed over a period of days to decades. The Δ_{LF} defined by Lloyd & Farquhar (1994) is thus a multiyear integrator of Δ. However, the autotrophic contribution to the isotope ratio of ecosystem respiration should respond to changes in moisture availability (as discrimination changes) and is likely to influence Δ_{LF} on a seasonal or interannual timescale. The

present estimates (Fig. 9) are based on half-hourly measurements, and are more indicative of short-term photosynthetic activity. Isotopic influences on the atmosphere are most significant during periods of strong flux. Thus the relevant discriminations are those when F_A is maximal in Fig. 7 (12.00–15.00 hours). Flux-weighted average discriminations for each case are shown in Table 3, and are similar for all cases, including Δ_{LF}. The flux-weighted discriminations obtained by the present measurements (16.8–17.1‰, or 18.1‰ for the long-term value) are at the low end of the typical C3 range, corresponding to C_i/C_a near 0.54–0.59 (Table 3 and Fig. 9). Error bars in Table 3 result from propagating the error of NEE, g_c, F_A, etc. The large variability in these parameters translates to large variability in flux-weighted discrimination (using standard errors instead of standard deviations would decrease the error estimates in Table 3 by a factor of roughly $\sqrt{19}$).

Bakwin *et al*. (1998) used data from the NOAA global sampling network to estimate discrimination at regional scales. After fossil fuel contributions were removed, with $\delta^{13}C_a = -7.9$‰ and $\delta^{13}C_r = -24.4$‰ (tall towers in Wisconsin and North Carolina with large regions of C3 deciduous forest) or –24.7‰ (their mean value at north temperate latitudes), they obtained estimates for Δ_{LF} of 16.5–16.8‰, which are in direct agreement with the present results. Because the tall tower measurements sample large regional air masses, it is likely that Bakwin's results include some influence of C4 crop photosynthesis, which is abundant in the midwestern USA, and should lower the average regional discrimination relative to the Walker Branch results presented here.

Lloyd & Farquhar (1994) and Fung *et al*. (1997) modelled global discrimination at large scales with fairly different results for C3 vegetation averaged around latitudinal bands (17.8‰ and 20‰, respectively). The former study explicitly included mesophyll resistance in their model while the latter did not, and this difference was thought to explain the contrast in their results (Fung *et al*. 1997). However, the present contribution also ignores mesophyll resistance and the results are more consistent with those of Lloyd & Farquhar (1994). It should be stressed that direct comparison between the present localized measurements and these studies is difficult because of the large differences in spatial scale.

Isotopic equilibrium and the dependence of isoflux on NEE

The simultaneous solution of (1) and (6) requires their independence. At isotopic equilibrium, the isotopic effects of photosynthesis and respiration in an ecosystem would be equal and opposite. Removal of one mole of CO_2 by photosynthesis would enrich canopy air in $^{13}CO_2$ to the same degree that addition of one mole of respiratory CO_2 would decrease it. Formally, isotopic equilibrium can be defined by $\delta^{13}C_r = \delta^{13}C_a - \Delta$, over an appropriate time interval. If this equality holds, then (6) is linearly dependent on (1) and isoflux $= \delta^{13}C_r$ (NEE). Further, the ratio of the fluxes (isoflux/NEE) at equilibrium would be simply the Keeling intercept, $\delta^{13}C_r$. How does this ratio compare in the present case? To answer this question an expression for the ratio isoflux/NEE in terms of mean quantities needs to be derived.

Formally, the total vertical flux of $^{13}CO_2$ is described by

$$^{13}\mathrm{CO_2}\ \text{flux} = \overline{\rho w[^{13}\mathrm{CO_2}]} \tag{11}$$

which can be estimated (as an isoflux) using the standard isotopic approximation

$$\approx \overline{\rho w(\delta^{13}C_a)C}. \tag{12}$$

Expanding each term using Reynolds averaging, and using δ instead of $\delta^{13}C_a$ for clarity,

$$= \overline{\rho w C} = \overline{\rho(w + w')(\delta + \delta')(C + C')}. \tag{13}$$

Multiplying the terms, recognizing that the mean of a primed quantity is zero, and assuming $\overline{w}$ gives

$$= \rho(\overline{\delta})\overline{w'C'} + \rho(\overline{C})\overline{w'\delta'} + \overline{\rho w'\delta' C'}. \tag{14}$$

The assumption is made that $\delta = mC + b$, and thus $\overline{\delta} = m\overline{C} + b$ and $\delta' = mC'$. Substituting these terms into the flux equation gives

$$\text{eddy isoflux} = (2m\overline{C} + b)\rho\overline{w'C'} + m\rho\overline{w'C'C'}. \tag{15}$$

Thus the eddy isoflux of $^{13}CO_2$ is a function of the total eddy flux of CO_2, the mean CO_2 mole fraction during the measurement period ($\overline{C}$), and a triple moment term. The first term on the right-hand side of the equation is typically two orders of magnitude larger than the triple moment term (data not shown), so the eddy isoflux can be well-approximated by the mean quantities

$$\text{eddy isoflux} \approx (2m\overline{C} + b)\rho\overline{w'C'}. \tag{16}$$

The ratio of eddy isoflux/total CO_2 flux in this case is proportional to $2m\overline{C} + b$. This ratio is not constant but varies over a diurnal cycle with the mean ambient CO_2 mole fraction $\overline{C}$, which implies that the isotopic composition of net CO_2 flux is not constant over a diel period. A plot of isoflux/NEE (which adds the further complication of storage fluxes) from Fig. 3(a),(b) follows this

relationship very closely (not shown), varying about a mean near the Keeling plot intercept.

Ideally, isotopic fluxes can be measured directly with the eddy covariance technique, but at present this is impossible for isotopes of CO_2. Thus, indirect approaches need to be used to estimate the isoflux (such as eqn 7). As noted above, the linear relation and the use of (7) appears robust. However, the distinction between this relation and the Keeling (1958) equation

$$\delta^{13}C_a = \text{slope}/C + \delta^{13}C_r \quad (17)$$

is subtle but potentially very important. It is unclear which equation is a better predictor of $\delta^{13}C$ based on C within the typical range of atmospheric CO_2 (see regressions in Table 2 and Bowling *et al*. 1999a).

Instead, in a fashion similar to (7), the Keeling equation could be used to estimate $\delta^{13}C_a$, and then calculate $^{13}CO_2$ eddy isoflux. Keeling's approach was intended originally to be used only at night, and assumes mixing of background CO_2 at sunset with respired CO_2 having a *single* isotopic composition throughout the night. Using (17) to predict $\delta^{13}C_a$ during the daytime assumes that all isotopic variation comes from a single source, and *forces* isotopic equilibrium. In fact, substituting (17) into (14) in the derivation above yields the predicted eddy isoflux/total CO_2 flux = $\delta^{13}C_r$. In the absence of direct measurements of $^{13}CO_2$ flux, the partitioning approach outlined in this study is dependent on the assumptions made about the relationship between isotopic composition and CO_2 mole fraction. If, in fact, (17) is correct, then (6) is a multiple of (1). In this case perfect isotopic equilibrium exists, there is no unique information in ^{13}C, and $^{13}C/^{12}C$ measurements cannot be used to partition net ecosystem exchange.

However, most terrestrial ecosystems are unlikely to be in isotopic equilibrium with the present atmosphere. The long-term disequilibrium between soil organic matter and atmospheric CO_2 is now well established (Schimel *et al*. 1994; Bird *et al*. 1996; Trumbore 2000). The Keeling relationship appears strong for ^{13}C at night, and it is perhaps more appropriate to use it instead of $\delta^{13}C$-vs.-C during nocturnal periods (as here) to calculate $^{13}CO_2$ eddy isoflux. During the day, the isotopic effects of photosynthesis may be different than those of respiration. Although Flanagan *et al*. (1996) found little variation within a season in $\delta^{13}C_r$ in boreal forests, recent work in coniferous forests of Oregon and Washington, USA, shows large (2–6‰) within-site seasonal variation in $\delta^{13}C_r$, which correlates well with plant water status (Bowling, Fessenden and Ehleringer, unpubl. data). Whole-canopy photosynthetic discrimination appears to respond to moisture limitations in a manner consistent with leaf level observations. It is speculated that the isotope ratio of the heterotrophic component of ecosystem respiration (excluding the rhizosphere) is unlikely to change significantly based on short-term changes in photosynthetic discrimination, because the substrate for respiration does not change.

Gaudinski *et al*. (2000) used radiocarbon measurements to estimate that 59% of soil respiration at Harvard Forest was derived from carbon that resided in the plant/soil system for less than one year, and that the average age of carbon respired by heterotrophs was 8 years. If the heterotrophic component stays more or less constant, but the autotrophic component changes over a season or between years, then equilibrium is unlikely. Thus, a change in whole-canopy discrimination in response to moisture availability will alter the isotopic equilibrium of an ecosystem on a timescale of weeks to months. Direct measurements of $^{13}CO_2$ flux, rather than the indirect methods of Yakir & Wang (1996), Bowling *et al*. (1999a), and this study, are necessary to assess the validity of these assumptions.

Conclusions

In this study relevant theory has been developed and applied to measurements in a temperate deciduous forest in order to assess the utility of stable isotopes in ecosystem-scale studies of carbon dioxide and water vapour exchange. Stable isotopes of CO_2 can be used in combination with standard micrometeorological flux measurements to partition net ecosystem CO_2 exchange into photosynthetic and respiratory fluxes. Despite potential complications, the approach used was successful for $^{13}CO_2$ in a complex natural system. Expected diurnal patterns and magnitudes of F_A and F_R were obtained which were consistent with those from other approaches, and consistent with our understanding of these fluxes at the leaf level. Whole-canopy photosynthetic discrimination was lower than expected but was consistent with other estimates in the literature. This approach is quite sensitive to assessment of canopy conductance through its influence on Δ, and to assumptions made about the relationship between isotopic composition and CO_2 mole fraction.

Acknowledgements

We thank K. Wilson and D. Baldocchi for collecting and sharing their flux and meteorological data, D. Schindler and B. Logan for hard work and much enthusiasm in the field, and D. Yakir, J. White, J. Berry, J. Lloyd, P. Blanken and L. Scott for thoughtful discussions. C. Cook and G. Hund provided invaluable assistance with the isotopic measurements. This research was funded equally by TECO NSF grant IBN9814507 and the National Institute for Global Environmental Change through the U. S. Department of Energy (Cooperative Agreement DE-FC03–90ER61010). Any opinions, findings, and conclusions or

recommendations expressed in this publication are those of the authors and do not necessarily reflect the views of NSF or DOE.

References

Auble DL, Meyers TP (1992) An open path, fast response infrared absorption gas analyzer for H_2O and CO_2, *Boundary-Layer Meteorology*, **59,** 243–256.

Bakwin PS, Tans PP, White JWC, Andres RJ (1998) Determination of the isotopic ($^{13}C/^{12}C$) discrimination by terrestrial biology from a global network of observations. *Global Biogeochemistry and Cycles*, **12,** 555–562.

Baldocchi D (1997) Measuring and modelling carbon dioxide and water vapour exchange over a temperate broad-leaved forest during the 1995 summer drought, *Plant, Cell and Environment*, **20,** 1108–1122.

Baldocchi D, Collineau S (1994) The physical nature of solar radiation in heterogeneous canopies: spatial and temporal attributes. In: *Exploitation of Environmental Heterogeneity by Plants* (eds Caldwell MM, Pearcy RW), pp. 21–71. Academic Press, San Diego, CA.

Baldocchi DD, Harley PC (1995) Scaling carbon dioxide and water vapour exchange from leaf to canopy in a deciduous forest. II. Model testing and application. *Plant, Cell and Environment*, **18,** 1157–1173.

Baldocchi DD, Law BE, Anthoni PM (2000) On measuring and modeling energy fluxes above the floor of a homogeneous and heterogeneous conifer forest. *Agricultural and Forest Meteorology*, **102,** 187–206.

Baldocchi DD, Meyers TP (1998) On using eco-physiological, micrometeorological and biogeochemical theory to evaluate carbon dioxide, water vapor, and trace gas fluxes over vegetation: a perspective. *Agricultural and Forest Meteorology*, **90,** 1–25.

Baldocchi DD, Vogel CA, Hall B (1997) Seasonal variation of carbon dioxide exchange rates above and below a boreal jack pine forest. *Agricultural and Forest Meteorology*, **83,** 147–170.

Bird MI, Chivas AR, Head J (1996) A latitudinal gradient in carbon turnover times in forest soils. *Nature*, **381,** 143–146.

Blanken PD, Black TA, Neumann HH *et al.* (1998). *Boundary-Layer Meteorology*, **89,** 109–140.

Bousquet P, Peylin P, Ciais P, Ramonet M, Monfray P (1999) Inverse modeling of annual atmospheric CO_2 sources and sinks 2. Sensitivity study. *Journal of Geophysical Research*, **104,** 26,179–26,193.

Bowling DR, Baldocchi DD, Monson RK (1999a) Dynamics of isotopic exchange of carbon dioxide in a Tennessee deciduous forest. *Global Biogeochemical Cycles*, **13,** 903–922.

Bowling DR, Delany AC, Turnipseed AA, Baldocchi DD, Monson RK (1999b) Modification of the relaxed eddy accumulation technique to maximize measured scalar mixing ratio differences in updrafts and downdrafts. *Journal of Geophysical Research*, **104,** 9121–9133.

Brooks JR, Flanagan LB, Varney GT, Ehleringer JR (1997) Vertical gradients in photosynthetic gas exchange characteristics and refixation of respired CO_2 within boreal forest canopies. *Tree Physiology*, **17,** 1–12.

Brooks JR, Hinckley TM, Ford ED, Sprugel DG (1991) Foliage dark respiration in *Abies amabilis* (Dougl.) Forbes: variation within the canopy. *Tree Physiology*, **9,** 325–338.

Buchmann N, Brooks JR, Flanagan LB, Ehleringer JR (1998) Carbon isotope discrimination of terrestrial ecosystems. In: *Stable Isotopes, Integration of Biological, Ecological, and Geochemical Processes* (ed. Griffiths H), pp. 203–221. BIOS Scientific, Oxford.

Buchmann N, Kao W-Y, Ehleringer JR (1996) Carbon dioxide concentrations within forest canopies – variation with time, stand structure, and vegetation type. *Global Change Biology*, **2,** 421–432.

Ciais P, Tans PP, White JWC *et al.* (1995) Partitioning of ocean and land uptake of CO_2 as inferred by $\delta^{13}C$ measurements from the NOAA Climate Monitoring and Diagnostics Laboratory Global Air Sampling Network. *Journal of Geophysical Research*, **100,** 5051–5070.

Davidson EA, Belk E, Boone RD (1998) Soil water content and temperature as independent or confounded factors controlling soil respiration in a temperate mixed hardwood forest. *Global Change Biology*, **4,** 217–227.

Duranceau M, Ghashghaie J, Badeck F, Deleens E, Cornic G (1999) $\delta^{13}C$ of CO_2 respired in the dark in relation to $\delta^{13}C$ of leaf carbohydrates in *Phaseolus vulgaris* L. under progressive drought. *Plant, Cell and Environment*, **22,** 515–523.

Ehleringer JR, Buchmann N, Flanagan LB (2000) Carbon isotope ratios in belowground carbon cycle processes. *Ecological Applications*, **10,** 412–422.

Ehleringer JR, Cook CS (1998) Carbon and oxygen isotope ratios of ecosystem respiration along an Oregon conifer transect: preliminary observations based on small-flask sampling. *Tree Physiology*, **18,** 513–519.

Ellsworth DS, Reich PB (1993) Canopy structure and vertical patterns of photosynthesis and related leaf traits in a deciduous forest. *Oecologia*, **96,** 169–178.

Evans JR, Sharkey TD, Berry JA, Farquhar GD (1986) Carbon isotope discrimination measured concurrently with gas exchange to investigate CO_2 diffusion in leaves of higher plants. *Australian Journal of Plant Physiology*, **13,** 281–292.

Farquhar GD, Ehleringer JR, Hubick KT (1989) Carbon isotope discrimination and photosynthesis. *Annual Review of Physiological Plant Molecular Biology*, **40,** 503–537.

Farquhar GD, O'Leary MH, Berry JA (1982) On the relationship between carbon isotope discrimination and the intercellular carbon dioxide concentration in leaves. *Annual Review of Plant Physiology and Plant Molecular Biology*, **9,** 121–137.

Flanagan LB, Brooks JR, Varney GT, Berry SC, Ehleringer JR (1996) Carbon isotope discrimination during photosynthesis and the isotope ratio of respired CO_2 in boreal forest ecosystems. *Global Biogeochemical Cycles*, **10,** 629–640.

Flanagan LB, Brooks JR, Varney GT, Ehleringer JR (1997) Discrimination against $C^{18}O^{16}O$ during photosynthesis and the oxygen isotope ratio of respired CO_2 in boreal forest ecosystems. *Global Biogeochemical Cycles*, **11,** 83–98.

Francey RJ, Tans PP, Allison CE, Enting IG, White JWC, Trolier M (1995) Changes in oceanic and terrestrial uptake since 1982. *Nature*, **373,** 326–330.

Friedli H, Siegenthaler U, Rauber D, Oeschger H (1987) Measurements of concentration, $^{13}C/^{12}C$ and $^{18}O/^{16}O$ ratios of tropospheric carbon dioxide over Switzerland. *Tellus*, **39B,** 80–88.

Fung I, Field CB, Berry JA *et al.* (1997) Carbon 13 exchanges between the atmosphere and the biosphere. *Global Biogeochemical Cycles*, **11,** 507–533.

Garten CT, Taylor GE Jr (1992) Foliar $\delta^{13}C$ within a temperate deciduous forest: spatial, temporal, and species sources of variation. *Oecologia*, **90,** 1–7.

Gaudinski JB, Trumbore SE, Davidson EA, Zheng S (2000) Soil carbon cycling in a temperate forest: radiocarbon-based estimates of residence times, sequestration rates and partitioning of fluxes. *Biogeochemistry*, in press:.

Goulden ML, Munger JW, Fan S-M, Daube BC, Wofsy SC (1996) Measurements of carbon sequestration by long-term eddy covariance: methods and a critical evaluation of accuracy, *Global Change Biology*, **2,** 169–182.

Grace J, Lloyd J, McIntyre J *et al.* (1995) Fluxes of carbon dioxide and water vapour over an undisturbed tropical forest in south-west Amazonia. *Global Change Biology*, **1,** 1–12.

Granier A, Biron P, Lemoine D (2000) Water balance, transpiration, and canopy conductance in two beech stands. *Agricultural and Forest Meteorology*, **100,** 291–308.

Greco S, Baldocchi DD (1996) Seasonal variations of CO_2 and water vapour exchange rates over a temperate deciduous forest. *Global Change Biology*, **2,** 183–197.

Harwood KG, Gillon JS, Griffiths J, Broadmeadow MSJ (1998) Diurnal variation of $\Delta^{13}CO_2$, $\Delta C^{18}O^{16}O$, and evaporative site enrichment of $\delta H_2{}^{18}O$ in *Piper aduncum* under field conditions in Trinidad. *Plant, Cell and Environment*, **21,** 269–283.

Hoefs J (1997) *Stable Isotope Geochemistry*. Springer, Berlin.

Hollinger DY, Kelliher FM, Byers JN, Hunt JE, McSeveny TM, Weir PL (1994) Carbon dioxide exchange between an undisturbed old-growth temperate forest and the atmosphere. *Ecology*, **75,** 134–150.

Hubbard RM, Bond BJ, Ryan MG (1999) Evidence that hydraulic conductance limits photosynthesis in old *Pinus ponderosa* trees. *Tree Physiology*, **19,** 165–172.

Jarvis PG, McNaughton KG (1986) Stomatal control of transpiration: scaling up from leaf to region. *Advances in Ecological Research*, **15,** 1–49.

Keeling CD (1958) The concentrations and isotopic abundances of atmospheric carbon dioxide in rural areas. *Geochimica et Cosmochimica Acta*, **13,** 322–334.

Kelliher FM, Leuning R, Raupach MR, Schulze E-D (1995) Maximum conductances for evaporation from global vegetation types. *Agricultural and Forest Meteorology*, **73,** 1–16.

Kòppers M, Schulze E-D (1985) An empirical model of net photosynthesis and leaf conductance for the simulation of diurnal courses of CO_2 and H_2O exchange. *Australian Journal of Plant Physiology*, **12,** 513–526.

Larcher W (1995) *Physiological Plant Ecology*. Springer, Berlin.

Lavigne MB, Ryan MG, Anderson DE *et al.* (1997) Comparing nocturnal eddy covariance measurements to estimates of ecosystem respiration made by scaling chamber measurements at six coniferous boreal sites. *Journal of Geophysical Research*, **102,** 28,977–28,985.

Law BE, Ryan MG, Anthoni PM (1999) Seasonal and annual respiration of a ponderosa pine ecosystem. *Global Change Biology*, **5,** 169–182.

Lenschow DH, Mann J, Kristensen L (1994) How long is long enough when measuring fluxes and other turbulence statistics? *Journal of Atmospheric and Oceanic Technology*, **11,** 661–673.

Lin G, Ehleringer JR (1997) Carbon isotopic fractionation does not occur during dark respiration in C_3 and C_4 plants. *Plant Physiology*, **114,** 391–394.

Lloyd J, Farquhar GD (1994) ^{13}C discrimination during CO_2 assimilation by the terrestrial biosphere. *Oecologia*, **99,** 201–215.

Lloyd J, Krujit B, Hollinger DY *et al.* (1996) Vegetation effects on the isotopic composition of atmospheric CO_2 at local and regional scales: theoretical aspects and a comparison between rain forest in Amazonia and a boreal forest in Siberia. *Australian Journal of Plant Physiology*, **23,** 371–399.

Magnani F, Leonardi S, Tognetti R, Grace J, Borghetti M (1998) Modelling the surface conductance of a broad-leaf canopy: effects of partial decoupling from the atmosphere. *Plant, Cell and Environment*, **21,** 867–879.

Malhi Y, Nobre AD, Grace J, Krujit B, Pereira MGP, Culf A, Scott S (1998) Carbon dioxide transfer over a Central Amazonian rain forest. *Journal of Geophysical Research*, **103,** 31,593–31,612.

McNaughton KG, van den Hurk BJJM (1995) A Lagrangian revision of the resistors in the two-layer model for calculating the energy budget of a plant canopy. *Boundary-Layer Meteorology*, **74,** 261–288.

Moncrieff JB, Malhi Y, Leuning R (1996) The propagation of errors in long-term measurements of land-atmosphere fluxes of carbon and water. *Global Change Biology*, **2,** 231–240.

Nakazawa T, Murayama S, Toi M, Ishizawa M, Otonashi K, Aoki S, Yamamoto S (1997a) Temporal variations of the CO_2 concentration and its carbon and oxygen isotopic ratios in a temperate forest in the central part of the main island of Japan. *Tellus*, **49B,** 364–381.

Nakazawa T, Sugawara S, Inoue G, Machida T, Makshyutov S, Mukai H (1997b) Aircraft measurements of the concentrations of CO_2, CH_4, N_2O, and CO and the carbon and oxygen isotopic ratios of CO_2 in the troposphere over Russia. *Journal of Geophysical Research*, **102,** 3843–3859.

Randerson JT, Thompson MV, Field CB (1998) Linking ^{13}C-based estimates of land and ocean sinks with predictions of carbon storage from CO_2 fertilization of plant growth. *Tellus*, **51B,** 668–678.

Raupach MR (2000) Inferring biogeochemical sources and sinks from atmospheric concentrations: general considerations and applications in vegetation canopies. In: *Global Biogeochemical Cycles in the Climate System* (eds Schulze ED *et al.*). Academic Press, San Diego, CA.

Raupach MR, Finnigan JJ (1988) Single-layer models of evaporation from plant canopies are incorrect but useful, whereas multilayer models are correct but useless. *Australian Journal of Plant Physiology*, **15,** 705–716.

Raupach MR, Finnigan JJ, Brunet Y (1996) Coherent eddies and turbulence in vegetation canopies: the mixing-layer analogy. *Boundary-Layer Meteorology*, **78,** 351–382.

Roden JS, Pearcy RW (1993) The effect of flutter on the temperature of poplar leaves and its implications for carbon gain. *Plant, Cell and Environment*, **16,** 571–577.

Ruimy A, Jarvis PG, Baldocchi DD, Saugier B (1995) CO_2 fluxes over plant canopies and solar radiation: a review. *Advances in Ecological Research*, **26,** 1–68.

Ryan MG, Hubbard RM, Pongracic S, Raison RJ, McMurtrie RE (1996) Foliage, fine-root, woody-tissue and stand respiration in *Pinus radiata* in relation to nitrogen status. *Tree Physiology*, **16,** 333–343.

Schimel DS, Braswell BH, Holland EA *et al.* (1994) Climatic, edaphic, and biotic controls over storage and turnover of carbon in soils. *Global Biogeochemical Cycles*, **8,** 279–293.

Tans PP, Berry JA, Keeling RF (1993) Oceanic $^{13}C/^{12}C$ observations: a new window on ocean CO_2 uptake. *Global Biogeochemical Cycles*, **7,** 353–368.

Tenhunen JD, Lange OL, Gebel J, Beyschlag W, Weber JA (1984) Changes in photosynthetic capacity, carboxylation efficiency,

and CO_2 compensation point associated with midday stomatal closure and midday depression of net CO_2 exchange of leaves of *Quercus suber*. *Planta*, **162,** 193–203.
Trolier M, White JWC, Tans PP, Masarie KA, Gemery PA (1996) Monitoring the isotopic composition of atmospheric CO_2: measurements from the NOAA global air sampling network. *Journal of Geophysical Research*, **101,** 25,897–25,916.
Trumbore S (2000) Age of soil organic matter and soil respiration: radiocarbon constraints on belowground C dynamics. *Ecological Applications*, **10,** 399–411.
Wilson KB, Baldocchi DD (2000) Seasonal and interannual variability of energy fluxes over a broadleaved temperate deciduous forest in North America. *Agricultural and Forest Meteorology*, **100,** 1–18.
Wilson KB, Hanson PJ, Baldocchi DD (2000) Factors controlling evaporation and energy partitioning beneath a deciduous forest over an annual cycle. *Agricultural and Forest Meteorology*, **102,** 83–103.
Wofsy SC, Goulden ML, Munger JW *et al.* (1993) Net exchange of CO_2 in a mid-latitude forest. *Science*, **260,** 1314–1317.
Yakir D, Wang X-F (1996) Fluxes of CO_2 and water between terrestrial vegetation and the atmosphere estimated from isotope measurements. *Nature*, **380,** 515–417.
Yang PC, Black TA, Neumann HH, Novak MD, Blanken PD (1999) Spatial and temporal variability of CO_2 concentration and flux in a boreal aspen forest. *Journal of Geophysical Research*, **104,** 27,653–27,661.
Yoder BJ, Ryan MG, Waring RH, Schoettle AW, Kaufmann MR (1994) Evidence of reduced photosynthetic rates in old trees. *Forest Science*, **40,** 513–527.

Appendix: solution of partitioning equations.

The formal combination of (1), (6), (8) and (9) can yield an equation for F_A. First, solving (9) for C_i/C_a, and substituting this into (8) yields

$$\Delta = b_R + (b_R - a)F_A/(g_c C_a). \quad \text{(A1)}$$

Next, this Δ is substituted into (6), and collecting like terms

$$\text{isoflux} = \delta^{13}C_R(F_R) + (\delta^{13}C_a - b_R)F_A - \left(\frac{b_R - a}{g_c C_a}\right)F_A^2. \quad \text{(A2)}$$

Multiplying (1) by $\delta^{13}C_R$ and subtracting from (A2) gives

$$\text{isoflux} - \delta^{13}C_R NEE = (\delta^{13}C_a - b_R - \delta^{13}C_R)F_A - \left(\frac{b_R - a}{g_c C_a}\right)F_A^2 \quad \text{(A3)}$$

which upon rearrangement yields the quadratic equation

$$-\left(\frac{b_R - a}{g_c C_a}\right)F_A^2 + (\delta^{13}C_a - b_R - \delta^{13}C_R)F_A + (\delta^{13}C_R NEE - \text{isoflux}) = 0. \quad \text{(A4)}$$

The solution to this equation is

$$F_A = \frac{-(\delta^{13}C_a - b_R - \delta^{13}C_R) \pm \sqrt{\frac{(\delta^{13}C_a - b_R - \delta^{13}C_R)^2 - 4(b_R - a)(\delta^{13}C_R NEE - \text{isoflux})}{g_c C_a}}}{2(a - b_R)/(g_c C_a)} \quad \text{(A5)}$$

and only one of the two roots yields a realistic value for F_A.